High-gradient Experiment on X-band Disk-Loaded Structures

T. Higo, T. Taniuchi, M. Yamamoto, J. Odagiri, S. Tokumoto,
H. Mizuno and K. Takata

KEK
Natinal Laboratory for High Energy Physics
1-1, Oho, Tsukuba, Ibaraki, 305 Japan

and

I. Wilson and W. Wuensch

CERN
European Organization for Nuclear Research
1211 Geneve 23, Switzerland

Abstract

The high-gradient performance of two travelling-wave X-band accelerating structures 20cm long has been studied. One of the structures, KEK, was conditioned up to an average accelerating gradient (Eav) of 68MV/m in 600 hours, while the other, CERN, reached 85MV/m in 50 hours. In the latter case the maximum output power was fed from the SLED system and the maximum field inside the structure was 138MV/m. This maximum level was limited by the available power from the klystron. Operation at the Eav=50MV/m level was found to be stable for both structures. The associated dark current at this level was less than a few μA for CERN but 20 to 30μA for KEK. Since the two electrical designs are almost the same the difference in dark current must be attributed to the difference in the two fabrication techniques. Modified Fowler-Northeim plots of downstream dark current showed a change of slope; a kink, around 50 to 60 MV/m above which the field enhancement factor was substantially increased.

Keywords: X-band, High gradient, Dark current, Breakdown

1. INTRODUCTION

In a linear collider such as the Japan Linear Collider(JLC)[1,2], acceleration via high-frequency accelerating structures is needed to save wall plug power while obtaining a very high energy. Furthermore, the accelerating field should be reasonably high in order to preserve the emittance through the linac and to make the length of the linac as small as possible. In the JLC main linac, accelerating fields of 50 to 100MV/m at the X-band are being considered.

In order to examine the possibility of such a high field acceleration, the breakdown limits of the standing-wave (SW) accelerating cavities in the S-band to X-band frequency range have been examined[3,4,5]. Though the results show a much higher field level than the above design field of the JLC, it is not obvious that such a high field can be obtained stably in a long travelling-wave (TW) structure given the difference between SW and TW operation. To study the characteristics in the TW case, high-field experiments on the TW structures were also performed at the S-band[6]. The experiments demonstrated the possibility of fields of 91MV/m at the S-band, though accompanied by a large amount of dark current of the order of mA. It was however found difficult to increase the field level further due to frequent breakdown even though this value was well below that estimated based on the breakdown limit obtained in the SW case. On the other hand, the amount of the dark current in this TW case[6] was the same as that of the 7-cell SW cavity experiment[7], even though the number of cells exposed to high field was by an order of magnitude larger. In addition, the amount of dark current as a function of surface field was found to obey a modified Fowler-Northeim formula above 60MV/m with roughly the same β values as those in the SW case.

As for the X-band, no elaborate study has been performed at KEK on the high-gradient characteristics of the TW structures. As a first step to these studies, a high-gradient experiment on an X-band accelerating structure, KEK, was comissioned in order to examine the possible field level of stable operation. Since the gradient considered at X-band for JLC ranges from values similar to the critical gradient of about 40MV/m [8] to more than twice of this value, one can easily imagine complicated mechanisms for the dark-current production and the breakdown characteristics. Therefore, various physical aspects, such as the amount of dark current, the energy spectra of the dark current, and the vacuum characteristics and so on were measured. Another structure (CERN) with almost the same electrical design, but fabricated at a different laboratory (CERN) in a different way, was also studied using the same experimental setup. Some of the results for these two structures have already been presented in a limited form[9,10]. Similar experiments are also being carried out at SLAC[11].

The experimental procedure and the results are described here in detail so that all necessary information is available for a meaningful comparison with similar experiments aimed at finding practical designs for a high gradient accelerator.

Some characteristics of the fabrication of the two structures and the experimental setup are first presented, then the conditioning procedure and the results are described in detail.

2. TESTED STRUCTURES

The two tested structures were almost the same in the electrical design. The constant impedance type of structure was chosen to prevent field-emitted electrons from hitting downward disks and making the production mechanism of the dark current more complicated. Each structure has 20 regular cells with 2 coupler cells. It is operated in the $2\pi/3$ mode at 11.4GHz. The relevant structure parameters are summarized in Table 1.

Table 1. Design parameters of the accelerating structure as calculated by SUPERFISH[12] or MAFIA[13].

Geometry	Param	KEK	CERN	[unit]
Beam hole radius	a	3	3	[mm]
Disk thickness	t	2	2	[mm]
Effective length(22 cells)	L	0.1924	0.1924	[m]
Group velocity	v_g/c	0.01177	0.0111	
Impedance	R/Q	15.74	16.0	[kΩ/m]
Shunt impedance	r	103.6	106.8	[MΩ/m]
Q value	Q	6584	6680	
Attenuation parameter	α	1.545	1.615	[neper/m]
Total attenuation	$\tau=\alpha L$	0.297	0.311	[neper]
Filling time	T_f	55	58	[ns]
Surface field enhancement	Ep/Eacc	3.91 / 2	3.91 / 2	

One of the structures (called KEK) was fabricated by KEK, while the other (called CERN) by CERN. Cross-sectional views of the two structures are shown in Figs. 1(a) and (b). The main differences between the two structures are summarized in Tables 2 and 3.

Table 2. Differneces in geometries between the two structures.

Part	KEK	CERN
Iris roundness	Straight edge	0.3mm
Iris thickness	~ 0.5mm	~ 2mm
Length of cutoff beam pipe	9.8mm	19.3mm
Waveguide height reduction	Quarter wave transformer	Taper

Table 3. Differeneces in fabrication method between the two structures.

Part	KEK	CERN
Material	C1011 *	C101#
Machining	Precision lathe	Ultra-precision lathe
Surface roughness	0.2μm	0.02μm
Coupler cell	Gold brazing	Silver brazing
Regular cell	Silver brazing	Silver brazing
Coupler iris	Deform after brazing	Machining only
Surface cleaning	Alkali soak	CERN
Furnace	Hydrogen	Vacuum
Tuning atmosphere	Air	Air

* supplied by Furukawa electric co., Japan.
\# supplied by Outokumpu, Finland.

One of the geometrical differences between the two structures is the thickness of the iris between waveguide and coupler cell. That of CERN is about 2mm and rounded while that of KEK is 0.5mm with a sharp edge. The other main difference is the length of the beam pipe at each end of the structure as shown in the figure. The difference in the group velocity results from a small difference in the beam-hole shape of each disk.

Each cell of KEK was machined using an usual-quality precision lathe with a typical surface roughness of 0.2μm. The machined cells were cleaned in an alkali soak bath following the usual cleaning process for commertial vacuum components. The cells were then brazed in a hydrogen furnace and afterwards were dimple-tuned in air using the on-axis detuning rod sitting on the beam hole. In this structure, not only regular cells but also the flat wall of the coupler cell and waveguide irises were mechanically deformed after brazing.

The cell of CERN were machined by an ultra-precision lathe (Rank-Pneumo MSG 325) with a typical surface roughness of 0.02μm. These were then cleaned using CERN's usual procedure, brazed in a vacuum furnace and tuned by dimpling from the outer walls.

3. DEFINITIONS

Eav in the flat-pulse case

In this paper, the accelerating field averaged along the whole structure was cited as the nominal accelerating gradient (Eav). The field decays as exp(-αz) when it propagates along the structure, where α is the attenuation parameter. Eav is calculated for the flat-pulse case (or actually for the non-SLED case) as

$$E_{av,flat} = Ein \frac{1-\exp(-\tau)}{\tau} = Ein\ F(\tau),$$

where

$$Ein\ [MV/m] = 18.6 * \sqrt{Pin\ [MW]}\ .$$
$$F(\tau) = 0.865,$$

where τ is the total attenuation parameter of the structure and Ein the field at the input coupler cell.

Although the attenuation parameter τ, and therefore the factor F(τ), depend on the actual values of Q and v_g, wehave used the same value of F(τ), for both structures because the difference of 5% in τ gives less than a 1% change in F(τ).

Eav in the SLED case

The Eav for the case with SLED was calculated as follows. The output pulse from the SLED system is schematically shown in Fig. 2(a). The main part which contributes to the formation of the field in the structure is between points B and C in the figure. The field inside this structure becomes smaller due to both the decay of the input power in time and the decay while travelling along the structure. This situation is shown in the snap shots of the fields along the structure at various times in Fig. 2(b). For a structure with a small filling time, compared to the decay of the SLED output, as in the present case, the integrated field along the structure becomes maximum, Vmax, when the head of the RF pulse reaches the output coupler. The average field Eav is defined in this case to be Eav = Vmax / L, where L is the total length of the structure. In practice,

$$E_{av,SLED} = E_{in,t=0} * 0.616,$$

where $E_{in,t=0}$ is the field in the input coupler cell at the maximum power of the SLED output pulse.

Surface field Es

The surface field Es was assumed for both the flat-pulse case and the SLED case to be

$$Es = Eav * 3.91/2.0,$$

where the factor 3.91 is the field-enhancement factor calculated by SUPERFISH for the standing wave case. The question arises whether the average field along the structure Eav should be used for Es or whether the maximum field is a better choice. In any case, even if we use the maximum surface field within the structure (that in the input coupler cell), the field enhancement factor (b) in the modified Fowler-Northeim formula is only reduced by only a factor $F(\tau)=0.865$ for the flat-pulse case.

The field-emitted current by the RF field was analysed using the modified Fowler-Northeim formula (FN formula)[3],

$$\frac{I_f}{Es^{2.5}} = C \times \exp\left(\frac{-6.53 \times 10^9 \times \phi^{1.5}}{\beta \times Es}\right)$$

where I_f is field emission current, C a constant, ϕ a work function for Cu (4.5 [eV]) and β the field-enhancement factor.

Dark current or peak current

"Dark current" or "peak current" in the present paper was defined as the current occuring during the RF pulse and is the measured average Faraday cup current / (pulse length * repetition rate).

4. EXPERIMENTAL SETUP

The aim of the present experiment is to study the characteristics of the conditioning process and the status obtained. The RF power was generated by a klystron "XB-50K"[14] and was transported to the structure through a 5.5m long rectangular waveguide (WRJ10). For the final stage of the conditioning of the CERN structure, a SLED RF-pulse compression system[15] was incorporated as shown in Fig. 3(a). During conditioning, various quantities such as the RF pulse at the input and output ports, dark currents and associated photons, vacuum levels and gas components and so on were measured. All the equipment was placed on a common platform as shown in Fig. 3(b) and were surrounded by one-meter concrete blocks for radiation shielding. The various measuring devices are explained as follows.

Directional coupler (DC)

RF pulses were monitored through the directional couplers of the cross-waveguide type. The coupling was about 60dB and the directivity better than 23dB. They were located 60cm from the structure. The RF signal was transported outside the shielding vault through a 5m-long low-loss cable and detected by a Shottky diode "301B"[16].

Current transformer (CT-UP and CT-DN)

Two current transformers "BS-20"[17] with an inner diameters of 16mm were used to measure the time structure of the dark current. The winding ratio was 10:1 and the time response was better than one nsec while the droop in 100nsec was negligibly small. The output was monitored by an oscilloscope using a 50Ω termination.

Faraday cup (FC-UP and FC-DN)

The average currents were measured by two Faraday cups having the same diameter as the beam pipe at upstream and downstream positions.

Profile monitor (PM)

The profile of the dark current was monitored with a profile monitor downstream of the structure. A 1.2mm thick luminescent ceramic plate "AF995R"[18] made of alumina ceramics doped with cromium oxide was placed at an angle of 45deg with respect to the structure axis. It was monitored by a TV camera.

Analyser magnet and a slit (AM, SL and FC)

The momentum spectra of the downward dark currents downstream were measured by an analyser dipole magnet with a Faraday cup behind slits made of 20mm thick stainless steel. The momentum acceptance in the present experiment was set at 4.3% for which the slit aperture was 10mm.

Scintillator (SC)

Five cylindrical plastic scintillators (SC1 to SC5), each 8mm in diameter and 20mm in length, were placed at equal spacing along the structure from input to output coupler cell. Each scintillator looked at the structure through a 12mm diameter hole which was drilled along the center of the lead block. The scintillators were therefore shielded in almost all directions except from behind. The distance between the cavity center axis and the scintillator was set to about 5cm. The output from the scintillator was guided through a light guide of 8mm in diameter and 1.5m in length to a photomultiplier tube for amplification. The tube is a "R329" integrated in the module "H1161"[19]. The anode current was monitored by an oscilloscope at the 50Ω termination.

The time delay in this system was estimated as being the sum of the delay of about 10ns in the light guide and 55ns due to the rise time and the transit time needed for amplification in the photomultiplier tube when operated at an applied voltage of about 1.1kV. The difference of the time delays among the photomultipliers is estimated to be less than 5ns since the sensitivity of the delay to the applied voltage was 2ns/100V.

TV monitor (TV)

Each iris (at input or output coupler cell) was monitored by a TV camera through the window in the H-corner bend of a waveguide located 40cm from the structure.

The distance between the devices for the dark-current measurement devices and the structure are listed in Table. 3- these are inportant when discussing the acceptance of the dark current. The relevant measuring devices described above were aligned with a precision better than 1mm with respect to the structure.

Table 3. Distance from input (output) coupler cell to various devices. All units are in mm.

Device	Distance	Aperture
CT-UP	100	ϕ16
FC-UP	430	ϕ36
PM	150	ϕ36
CT-DN	300	ϕ16
AM	660	24w × 24h
FC-DN	1130	ϕ36

Vacuum pumping (IP and G)

The structure was evacuated by four 20 liter/sec ion pumps (IP) through two irises and the beam pipes at both ends. The positions of the pumps are shown in Fig. 3(b). Vacuum levels were monitored by cold cathode gauges (CCG or simply G). Since all the gauges were attached to different sides of the waveguide or the beam pipe from those of the ion pumps they measured the vacuum level in the waveguide or beam pipe directly without being purturbed by the pumping speed of the ion pumps as long as the pumping by CCG gauge is negligibly small.

Table 4. Conductances of various components in the vacuum system.

Part	dimension [mm]	pumping speed [liter/sec]
Regular cell to cell	ϕ6 in each 8.75	2.4 (for 1 cell)
Input/output iris	5 × 7.5 × 0.5t	4
Waveguide to IP port	ϕ1.5 × 36	10
Waveguide	22.86w × 10.12h	0.6 (for 1m)
Cutoff beam pipe (KEK)	ϕ6 × 9.8 long	1.3
Cutoff beam pipe (CERN)	ϕ6 × 19.3 long	0.7
Beam duct	ϕ36	5.2 (for 1m)

In experiments on X-band structures, the vacuum conductances of various components are usually small due to the small component sizes. The conductances of various components of the experimental setup were estimated and are listed in Table 4. The vacuum level in the coupler cell is estimated to be about 5-times larger than that measured at the waveguide pumping port.

Conditioning control

Automatic conditioning control was performed using a VAX3500 through CAMAC. The RF power level was varied by changing the applied voltage to the klystron while monitoring the vacuum levels. When the vacuum or RF interlock activated, the next pulse was inhibited until the vacuum recovered.

5. EXPERIMENTAL RESULTS AND DISCUSSIION

Conditioning process

Parameters of the conditioning of the structures are listed in the following Table.

Table 5. Typical conditioning parameters.

Structure	Pulse width (ns)			Rep. Rate (Hz)		
	min	typical	max	min	typical	max
KEK	50	**50**	100	10	**50**	100
CERN	50	**100**	100	10	**50**	50

Typical pulse shapes of RF signals, CT outputs and scintillator outputs are shown in Fig. 4. The reflection of the RF from the structure was monitored and input RF was interrupted when the observed reflection was much higher than the stable condition. It should be noted that the two peakes in the reflection signal coresponding to reflection coefficient as large as 0.3 were due to the small bandwidth of the structure and the fast rise or fall times of the RF signal. Vacuum levels were also monitored and the input RF was

interrupted if any of them exceeded 10^{-4} Pa. Typical RF pulses with various pulse lengths are shown in Fig. 5 The RF pulse for SLED operation is shown in Fig. 6.

Conditioning history

The maximum accelerating field averaged along the structure Eav versus total number of shots is shown in Fig. 7. For the KEK case, 600 hours of conditioning and 6×10^7 shots were needed to reach the maximum field of 68MV/m. Conditioning with a long pulse width of 100nsec was needed for a while around the 55-60MV/m level after 3×10^7 shots to get over a particularly difficult power barrier (see points marked by crosses in Fig. 7). It was very difficult to increase the power level beyond the final point obtained due to frequent breakdowns in the structure. It should be noted that there was no power increase in the last 100-hours conditining at 50Hz. On the other hand, a maximum field of 89MV/m was obtained for the CERN case with only 50 hours, and less than 1×10^7 shots. This field level was limited by the available power from the klystron even incorporating the pulse compression by SLED.

Breakdown field versus pulse width

The breakdown limit of the KEK and CERN structures at various stages of conditioning are shown in Fig. 8. The maximum stable field level data as a function of pulse length (t) was best fitted by a $t^{-1/2}$ dependence.

Dark current versus average accelerating gradient

Plots of dark currents versus Eav for both structures at various stages of conditioning are shown in Figs. 9 and 11. Both the upstream and downstream dark current of KEK decreased monotonically by more than an order of magnitude during conditioning. Figs. 10 and 12 show the data in a modified Fower-Northeim plot[3]. The upstream data show linear behavior. The downstream data show a change of slope, a kink, at Eav=35 to 50 MV/m for the KEK structure and 60 MV/m for the CERN structure with a reduced field enhancement factor at higher fields. The phenomenon is probably related to the onset of dark current capture at the critical field of 40MV/m[8,20].

History of the dark current

The dark current generated in the KEK structure with an accelerating gradient of 50 MV/m at various stages of conditioning is shown in Fig. 13. The dark current was continuously decreased throughout the conditioning until the final stage. The dark current decreased even when the maximum field had ceased to increase as was the case represented in the last three points. Such a result suggests a different origin for dark current and breakdown. Field-enhancement factors as a function of the number of shots are shown in the same figure for the case of KEK. The field-enhancement factors β-UP and β-DN reached values 50 to 60 and are also shown in Fig. 13.

Comparison of the dark current of the two structures

The dark currents as a function of Eav at the final stage of conditioning for both structures are shown in Fig. 14. At 50 MV/m and a pulse length of 50ns the dark current of the KEK structure was more than 10 times larger than that of the CERN structure. This difference may reflect the different fabrication process since the electrical designs of both strucrures are the same. With a pulse length of 100ns the ratio increased to over 100. This

behaviour may reflect the difference in the final stage of conditioning between the two structures; the CERN structure was conditioned typically with a 100ns pulse width and reached a level well above 50MV/m at 100ns, the KEK structure however was conditioned typically with 50ns pulses for a faster increase of maximum field and was therefore far from being conditioned for 100ns pulses at the 50 MV/m level.

Peak current versus the pulse width

Peak current versus pulse width is shown in Fig. 16. Upstream dark current was roughly constant for pulse width longer than 25ns. This result suggests that this current comes mainly from the input coupler region and is continuously created during an entire RF pulse. The downstream current increased with pulse length up to one filling time and decreased thereafter. We would expect constant dark current above one filling time when the full length of the section contributes to the trapping process.The fact that for longer pulses it decreases can be explained by the decreasing relative contribution of the high frequency components of the rising and falling edges (see section - frequency dependence of dark current). As the pulse length is reduced below one filling time, the length over which trapping occurs is reduced and the level of dark current therefore falls. The data indicates that for very short pulses the higher dark current yield associated with the increased relative contribution of the high frequency component does not compensate for this decrease in trapping length.

Dark-current pulse shape

Typical dark-curent pulses are shown in Fig. 17 for 50ns pulse length. The main portion of the currents both upstream and downstream were centered around the time when the RF pulse had filled the structure. In this case, the pulse length happened to be the same as the filling time. The pulse shape did not vary appreciablly by changing the field level Eav.

Frequency dependence of the dark current

The amount of the dark current is plotted versus the operating frequency in Fig. 18. As shown in this figure, the increase in the upstream dark current was rather small showing the increase of the field in coupler cell to be small, while the increase of the downstream dark current is very large as the π mode was approached. This phenomenon is the same as that observed at SLAC[11].

Dark-current spot size

In the early stage of conditioning, the profile monitorshowed lots of small spots jittering from pulse to pulse and scattered all over the beam duct. Below the maximum conditioned level, the spot became stable. A typical stable profile of the dark current is shown in Fig. 19. The shape was found to be the same for both structures and in both the SLED and non-SLED cases. The stable spot size and position did not move, the core of the spot being ellipsoidal with a horizontal width of 1.5cm and a vertical width of 1cm. In the later part of conditioning, there was usually only the stable spot with sudden flashes spreading all over the screen when breakdown occured preceded sometimes by weaker flushes, indicating pre-breakdown phenomena.

Momentum spectrum of the downstream dark current

The momentum spectra of the dark current from KEK are shown in Fig. 20. For pulse lengths shorter than the filling time of the structure, there were peaks around a few to several

MeV/c without any noticeable plateau. As the pulse length was increased above the filling time, a plateau emerged up to a maximum energy point corresponding to in phase acceleration along the entire structure.

Momentum spectra of the dark current from CERN are shown in Fig. 21 for various pulse lengths. The spectral change with pulse length seems complex. The momentum spectrum with SLED in operation is shown in Fig. 22. The end point of the spectrum was in agreement with the maximum possible acceleration.

The momentum spectra for both structures are compared in Fig. 23. A large amount of low-enegy dark current was observed in the KEK case but not in the CERN case. Even though the electrical parameters are almost the same they were fabricated differently. If such a dark current is harmful, the difference of fabrication should be studied in detail.

Scintillator output pulse shape

Typical scintillator outputs are shown in Fig. 24 for stable operating conditions for three different pulse widths. The figures in the left-hand side were taken in the single-shot mode while those in the right show the envelope of several tens of shots. It was found that the timings of the scintillator signals were scattered from pulse to pulse but they were always occured in the period between the time the head of the RF pulse reached the output port and the tail of the RF pulse reached the input port, that means they.were generated during the structure was fully filled with RF.

Breakdown patterns

Two typical breakdown patterns are shown in Fig. 25. It should be noted that almost all the breakdowns throughout the conditioning of both structures could be categorized into these these two types.

Vacuum characteristics

The base vacuum level was rather stable during the conditioning except when the maximum field level was increasing rapidly in which case increases of the vacuum level by almost an order of magnitude occured from time to time. The base vacuum levels at the waveguide of the input port , at the waveguide of the output port and at the beam line were 1.3×10^{-5}, 0.6×10^{-5} and 0.2×10^{-5} [Pa], respectively. The increase of the vacuum level with the RF on was very small. The base vacuum level was therefore determined by the outgassing rate without RF and the pumping speed. The estimated maximum vacuum level inside the structure was about 1×10^{-4} Pa at the input coupler cell.

The output of the quadrupole residual gas mass analyser is shown in Fig. 26. As seen in the figure, typical mass numbers were 2, 14, 16, 17, 18, 20, 28, 40 and 44. There was no drastic change between RF on and off except for the amount of the hydrogen peak.

6. SUMMARY AND CONCLUSIONS

Two 20cm X-band accelerating structures were conditioned and their characteristics under high field operation were studied.

One of the structures, KEK, was conditioned up to an average accelerating gradient Eav of 68MV/m in 600 hours, while the other, CERN, reached 85MV/m in 50 hours. In the latter case the maximum output power was fed from the SLED system and the maximum field inside the structure was 138MV/m. This maximum level was limited by the available power from the klystron. Operation at the Eav=50MV/m level was found to be stable for both structures. The associated dark current at this level was less than a few μA for CERN

but 20 to 30μA for KEK. Since the two electrical designs are almost the same the difference in dark current must be attributed to the difference in the two fabrication techniques. Modified Fowler-Northeim plots of downstream dark current showed a change of slope, a kink, around 50 to 60 MV/m above which the field enhancement factor was substantially increased.

The following table summarizes some of the results at the final stage of the conditioning.

Table. 6 Results at the final stage of the conditioning.

Structure	[units]	KEK	CERN
Total conditioning time	[hours]	620	50
Total number of shots	[10^7]	6.2	0.85
Maximum average field	[MV/m]	68	85
kink point	[MV/m]	50	60
β downstream in FN plot			
100ns, above kink		#	91
100ns,below kink		41	24
50ns, above kink		64	179
50ns, below kink		36	70
Dark current downstream	[μA]		
at 50MV/m, 50ns	50ns	30	2
at 50MV/m,100ns	100ns	20*	0.1*

* estimated by an extrapolation, # could not be obtained.

ACKNOWLEDGEMENT

The authors would like to thank the members of ATF at KEK for offering us the test area and various hardware and software at the TRISTAN experimetal hall, "NIKKO". Special thanks should be expressed to Dr. H. Matsumoto for advice concerning various aspects based on his experiences involving high-gradient experiments at the S-band. Drs. Y. Yamazaki, S. Yamaguchi and T. Shintake are acknowledged for various useful discussions.

We would also like to thank Messrs. C. Achard and S. Leblanc for their help in the design and fabrication of the structure CERN.

The authors would like to thank Profs. Y. Kimura at KEK and W. Schnell at CERN for making the collaboration possible and for many useful and stimulating discussions.

I. Wilson and W. Wuensch thank the KEK management and staff for making their stay in Japan both enjoyable and successfull.

REFERENCES

[1] K. Takata, "Recent Progress in R&D Works for the Japan Linear Colider", XVth Int. Conf. High Energy Accelerator, Hamburg, Germany, July,1992, p811.

[2] JLC Group, "JLC-I", KEK-Report 92-16, Dec. 1992.

[3] G. A. Loew and J. W. Wang, "RF Breakdown Studies in Room Temperature Electron Linac Structures", XIII Int. Symposium on Discharges and Electrical Insulation in Vacuum, Paris, France, 1988, SLAC-PUB- 4647, 1988 and references therein.

[4] J. W. Wang, "RF PROPERTIES OF PERIODIC ACCELERATING STRUCTURES FOR LINEAR COLLIDERS", SLAC-Report-339, 1989.

[5] E. Tanabe, "Breakdown in High-Gradient Accelerator Cavities", Proc. 1984 Linear Accelerator Conference, p.403, Seeheim/Darmstadt, West Germany, 1984.
[6] H. Matsumoto et al., "High Gradient Experiment at the Accelerator Test Facility", XVth Int. Conf. High Energy Accelerator, Hamburg, Germany, July, 1992, p818. and KEK Pre-print 92-84, 1992.
[7] G. A. Loew, Third Int. Conf. on Linear Colliders, LC91, Protvino, USSR, 1991, p506.
[8] S. Yamaguchi, "Simulation studies on High-Gradient Experiments", LAL/RT 92-18, 1992.
[9] T. Higo et al., "High Gradient Experiment for X-band Travelling Wave Structure", 16th Int. Linac Conf., Ottawa, Canada, 1992 and KEK pre-print 92-99, 1992.
[10] T. Higo et al., "High Gradient Testing of an 11.4GHz Accelerating Structure for KEK/CERN Collider Studies", CLIC NOTE 187, 1993.
[11] J. Wang et al., "High-gradient studies on 11.4GHz copper accelerator structures", 16th Int. Linac conference, Ottawa, August 1992.
[12] K. Halbach and R. F. Holsinger, Particle Accelerator, 7 (1976) 213.
[13] K. Klatt et al., "MAFIA A-Three-Dimensional Electromagnetis CAD System for Magnets, RF Structures and Transient Wake-Field Calculations", Proc. 1986 Linear Accelerator Conf., SLAC-Report-303, 1986, p276-278.
[14] H. Mizuno et al., "X-band Klystron for Japan Linear Collider", KEK Preprint 90-90, 1990.
[15] S. Tokumoto et al., "X-band (11.424GHz) SLED System", 16th. Int. Linac Conf., Ottawa, Canada, Aug., 1992. and KEK Pre-print 92-115.
[16] Supplied by a company, KRYTAR, USA.
[17] Supplied by a company, Pulse Electronics, Japan.
[18] Supplied by a company, Demarquest, France.
[19] Supplied by HAMAMATU PHOTONICS K.K., Japan.
[20] R. Parodi, Presentation at 4th. Int. Conf. on Linear Colliders, LC92, Garmisch-Partenkirchen, Germany, 1992.

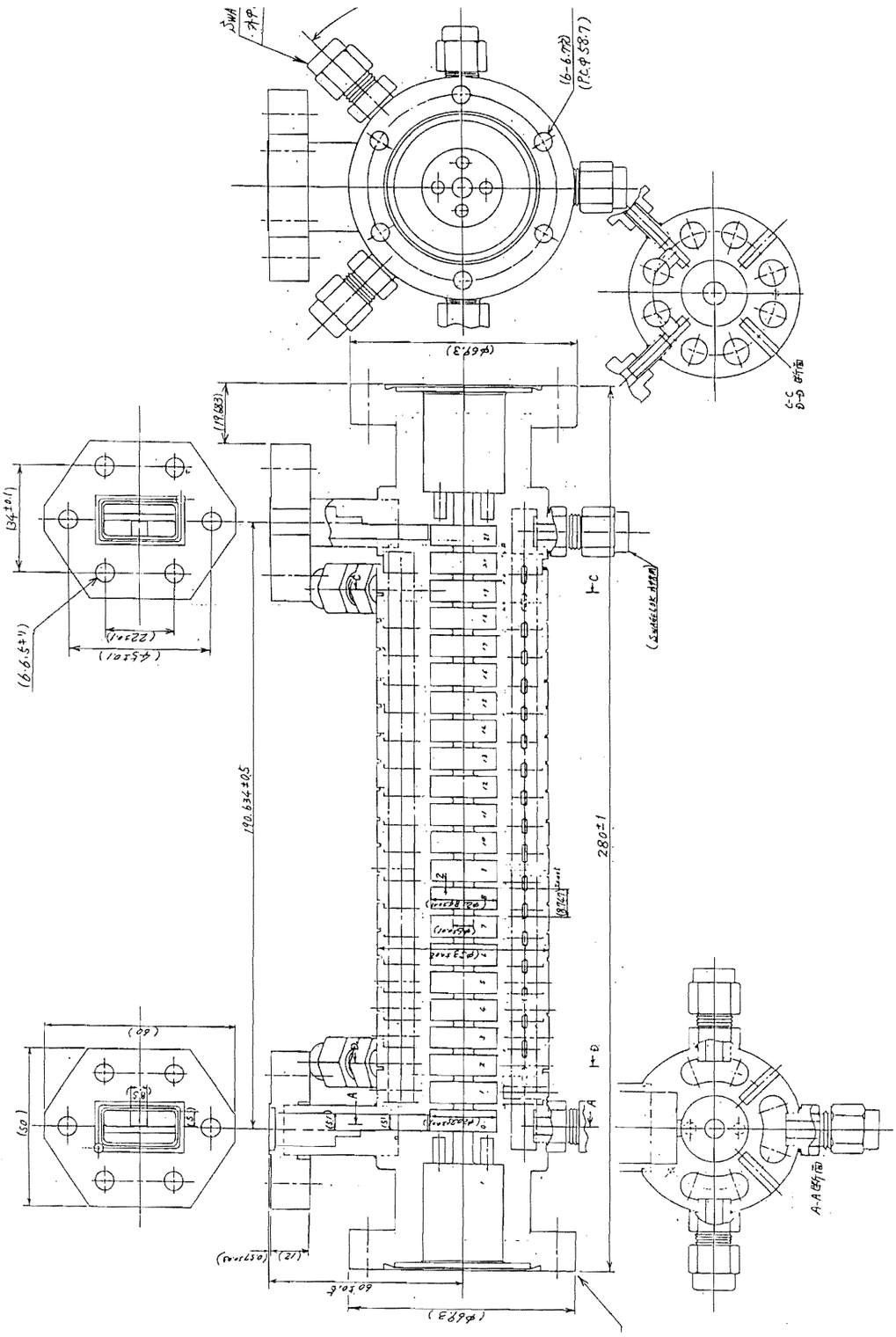

Fig. 1(a) Schematic drawing of "KEK".

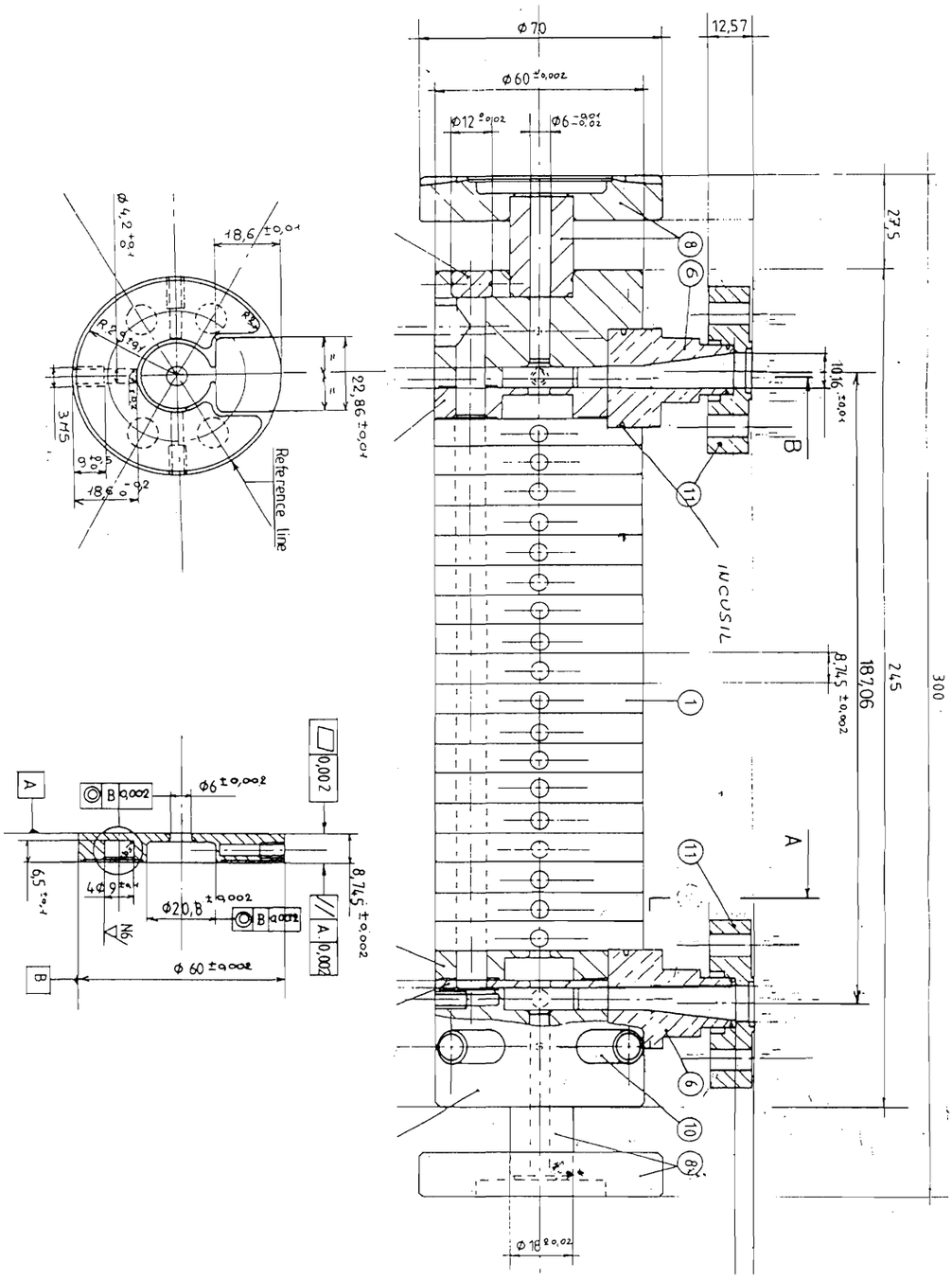

Fig. 1(b) Schematic drawing of "CERN".

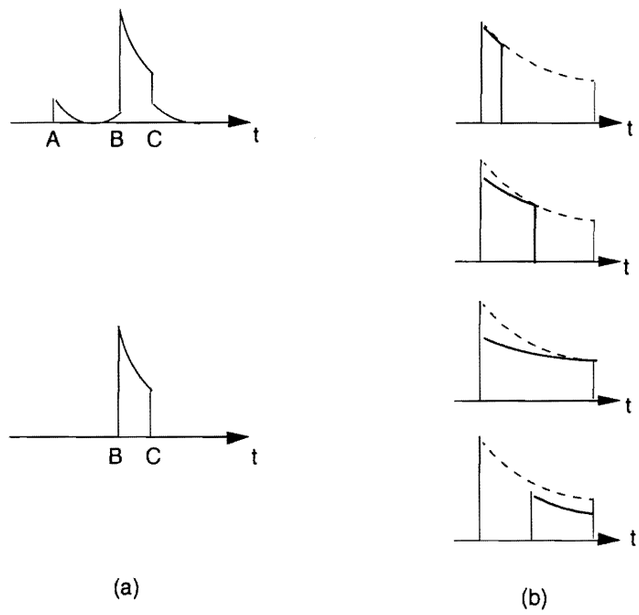

Fig. 2 Schematic diagram of the SLED pulse wave form. (a): Upper: SLED ideal output, lower: main part which is included in the estimation of the field inside the structure. (b): Snap shots of the field in the accelerating structure at various timing; from top to bottom, the beginning, less than the filling time, just at the filing time and later than the filing time.

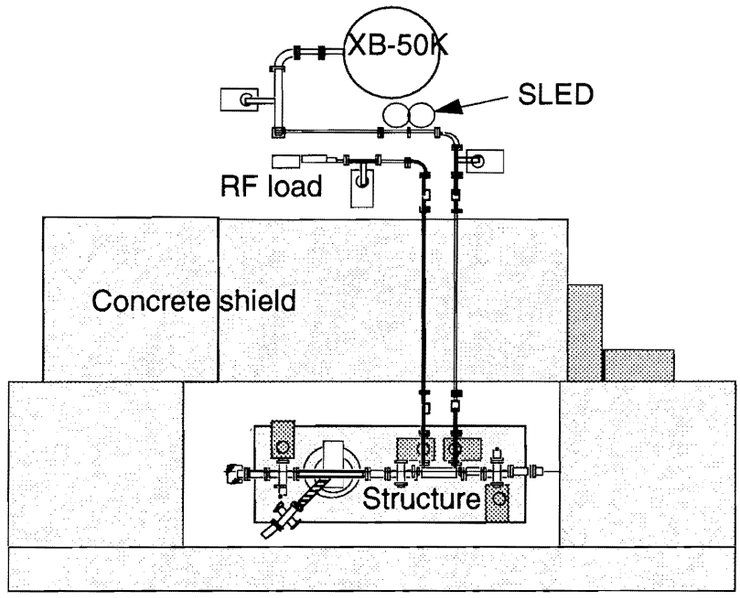

(a)

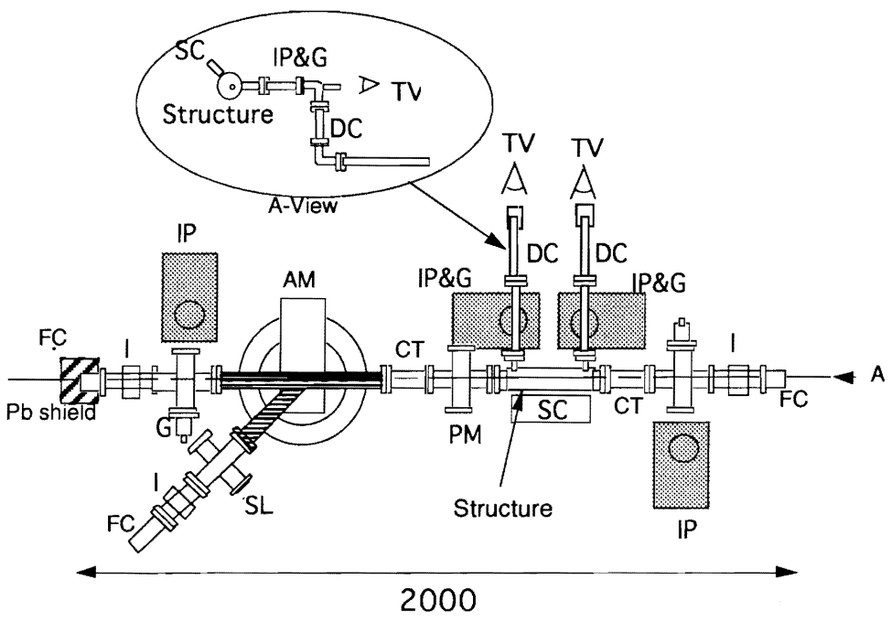

(b)

Fig. 3. Experimental setup. (a): Klystron, SLED, structure, RF load, etc. (b): setup in detail; CT:current transformer, FC: Faraday cup, AM: analyser magnet, SL: slits, I: insulating duct, SC: scintillation counter, DC: directional coupler, PM: profile monitor, IP: ion pump, G: cold cathode gauge, TV: TV monitor.

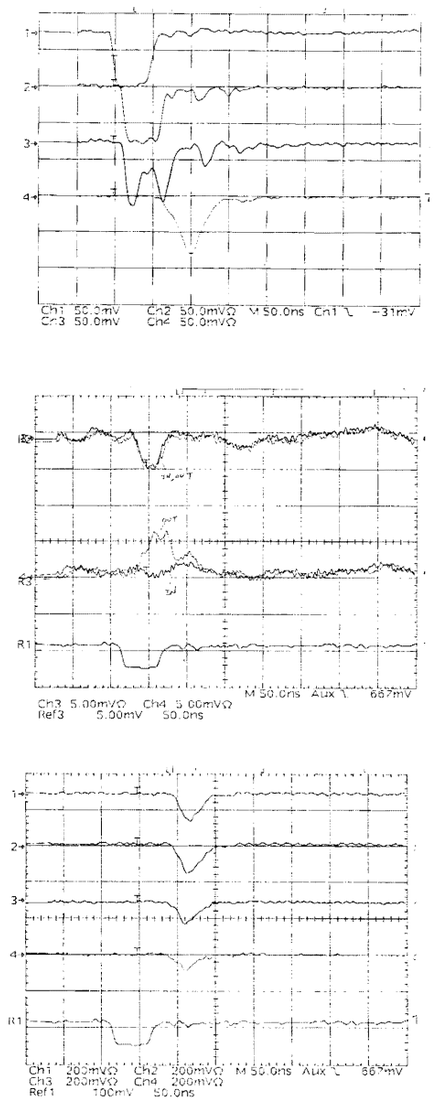

Fig. 4. Typical pulse shapes measured for "KEK". (a): RF pulse of klystron output, structure input, reflected from structure and transmitted from structure, respectively, from top to bottom. (b): CT outputs. Up trace is of CT-UP while that of middle CT-DN. Two traces in each CT signals are those with and without profile monitor inserted between the strucrture and the CT-DN. (c): Scintillation counter photomultiplier output. The top four traces are those from scintillator SC1,SC2,SC4 and SC5. The bottom trace in (b) and (c) show the input RF timing, the same as structure input RF .

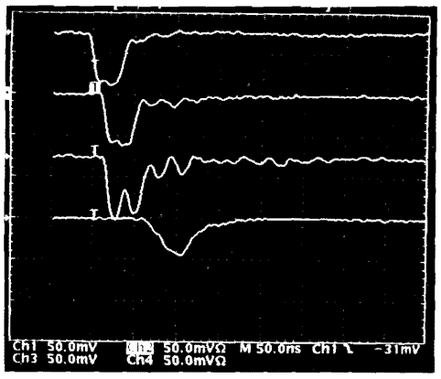

(a) 30ns

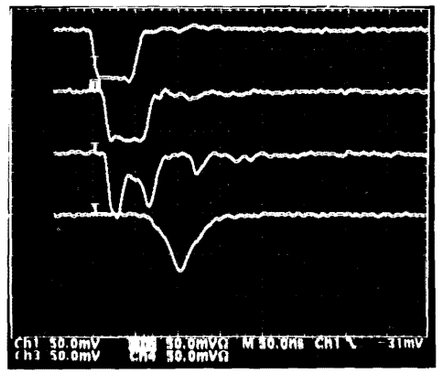

(b) 50ns

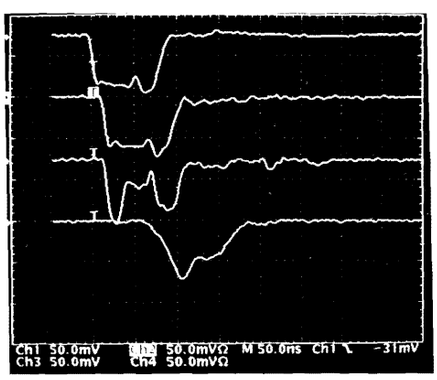

(c) 80ns

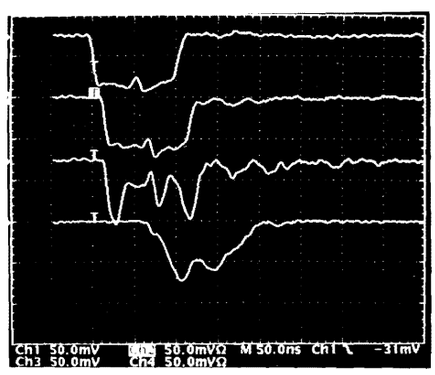

(d) 100ns

Fig. 5. Typical RF pulse shapes measured for "KEK" at the pulse length of (a) 30ns, (b) 50ns, (c) 80ns and (d) 100ns. Four traces in each picture are those of klystron output, structure input, reflected from structure and transmitted from structure, respectively from top to bottom.

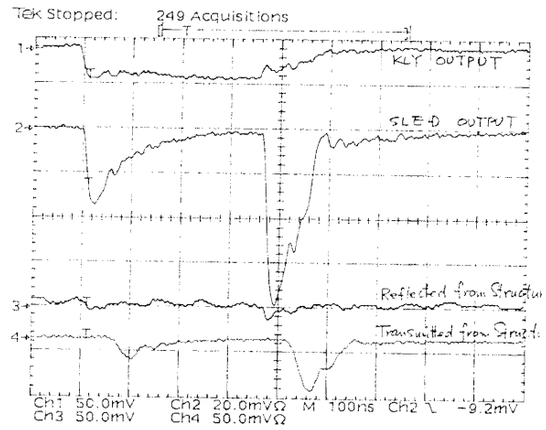

(a)

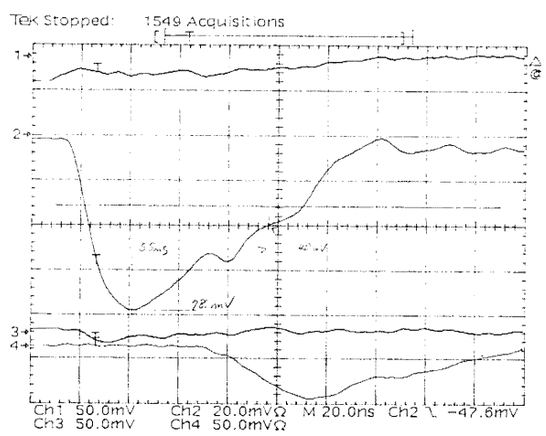

(b)

Fig. 6. Typical SLED pulse operated for feeding "CERN" structure. Four traces in each picture are RF pulse of klystron output, SLED output measured as structure input, reflected from structure and transmitted from structure, respectively, from top to bottom. The time scale in (a) is 100ns/div while (b) 20ns/div.

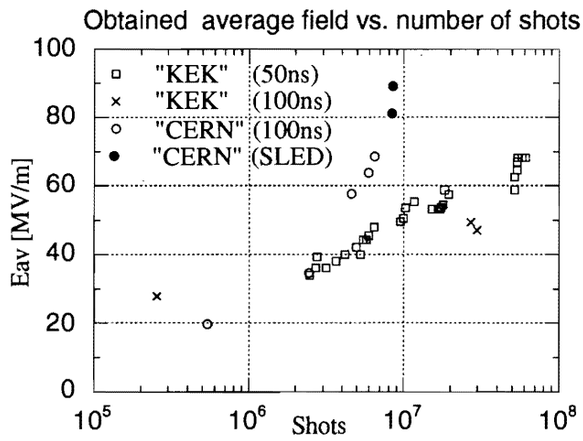

Fig. 7. Obtained average field versus number of shots.

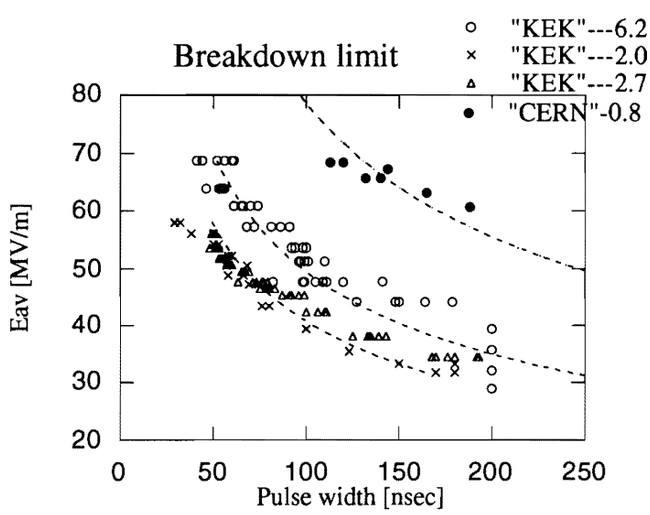

Fig. 8. Breakdown limit for "KEK" at various stage of the conditioning and that for "CERN" at the final stage of non-SLED conditioning. The numbers in the definition of the symbols are the number of shots up to then in the units of 10^7. Dotted lines show the dependence of (pulse width) $^{-1/2}$.

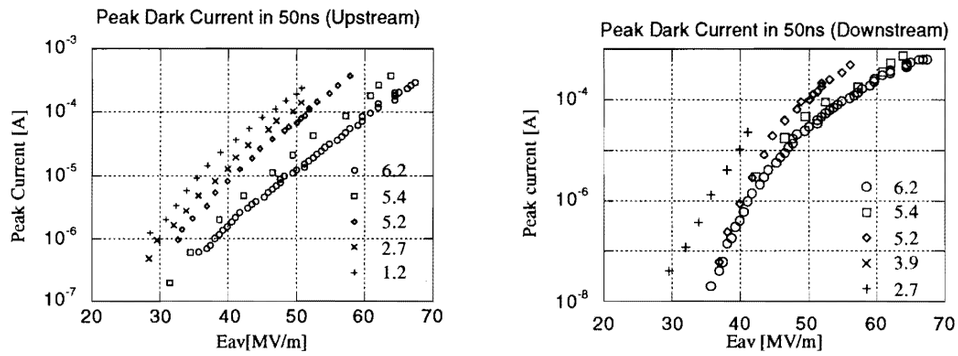

Fig. 9. Dark current versus average field at various stages in conditioning for "KEK" case. Pulse width is 50ns. Numbers to the right of each symbols are the integrated number of shots in units of 10^7.

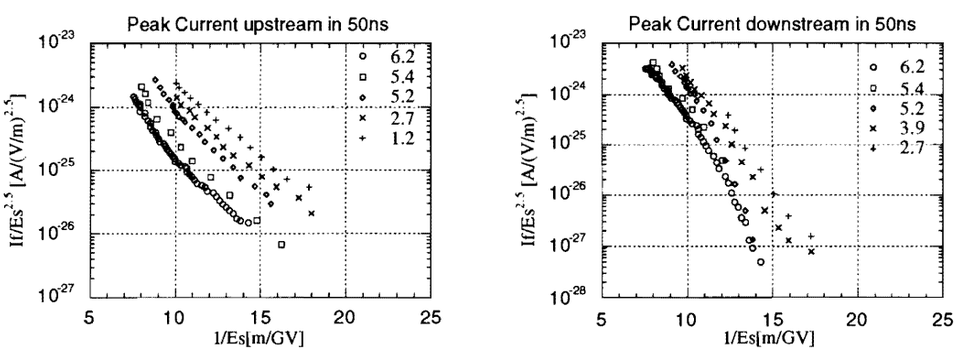

Fig. 10. Modified Fowler-Northeim plot at various stages of the conditioning of the "KEK" structure. Pulse width is 50nsec. Numbers to the right of each symbols are the intergated number of shots in units of 10^7.

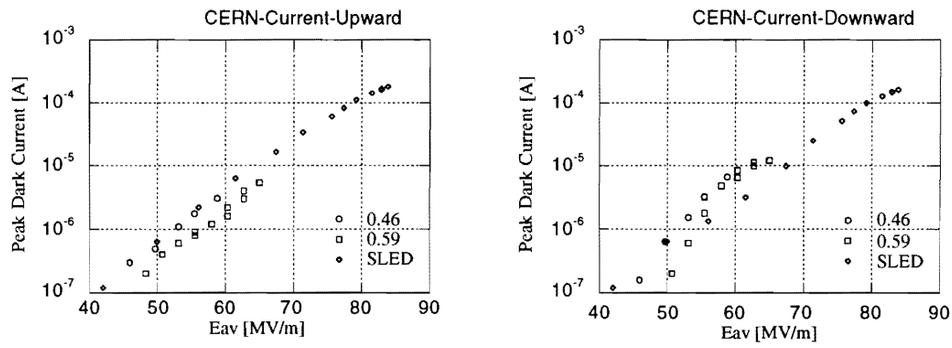

Fig. 11. Dark current versus average field at various stage in conditioning for "CERN" case. Pulse width is 100ns for non-SLED case. Numbers to the right of each symbols are the integrated number of shots in units of 10^7.

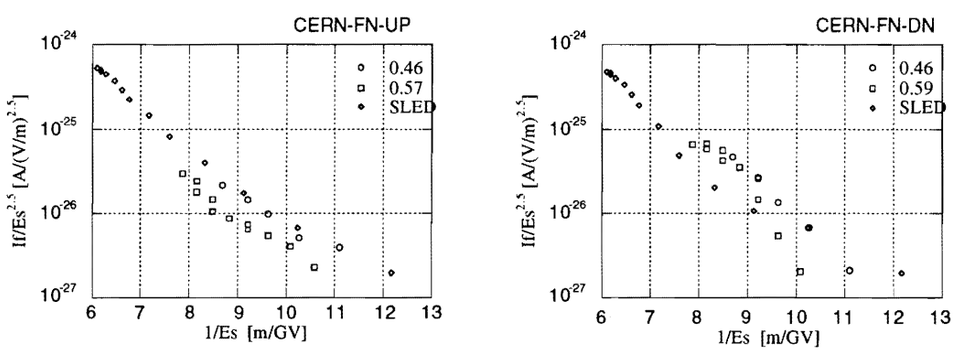

Fig. 12. Modified Fowler-Northeim plot at various stages of conditioning of the "CERN" structure. Pulse width is 100nsec for non-SLED case. Numbers to the right of each symbols are the integrated number of shots in units of 10^7.

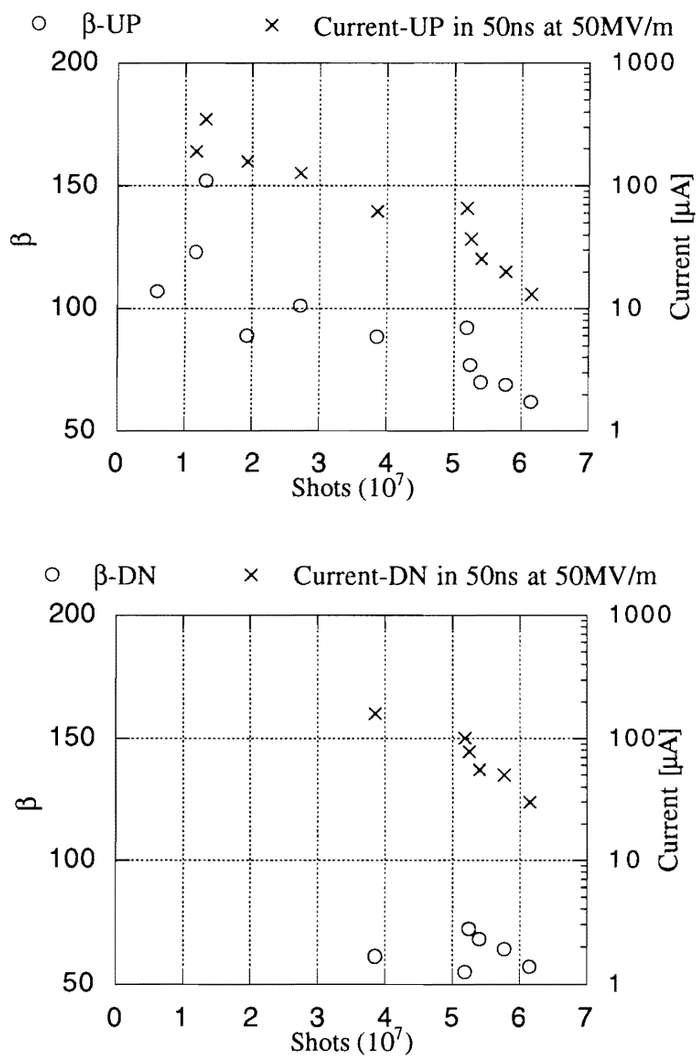

Fig. 13. Field enhancement factor β and the peak current at Eav=50MV/m in various stages of the conditioning of "KEK" structure. The β's were deduced from the data above the kink point in the modified Fowler-Northeim plot in Fig. 10.

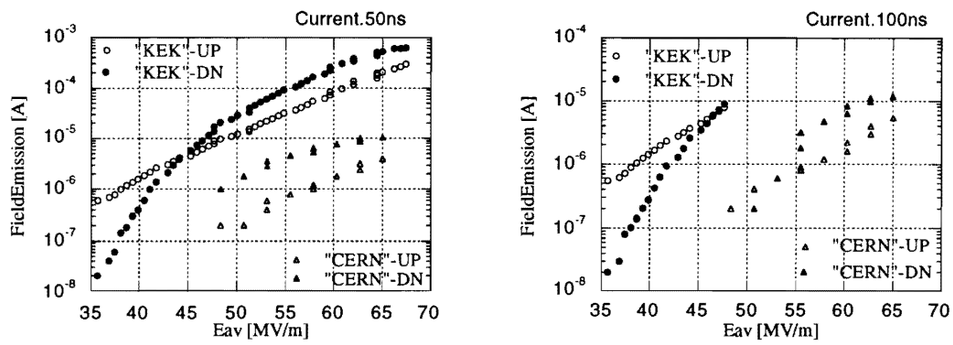

Fig. 14. Peak current versus Eav for "KEK" and "CERN" structure at the final stage of the conditioning without pulse compression. The pulse widths are 50ns and 100ns for upper and lower figure, respectively.

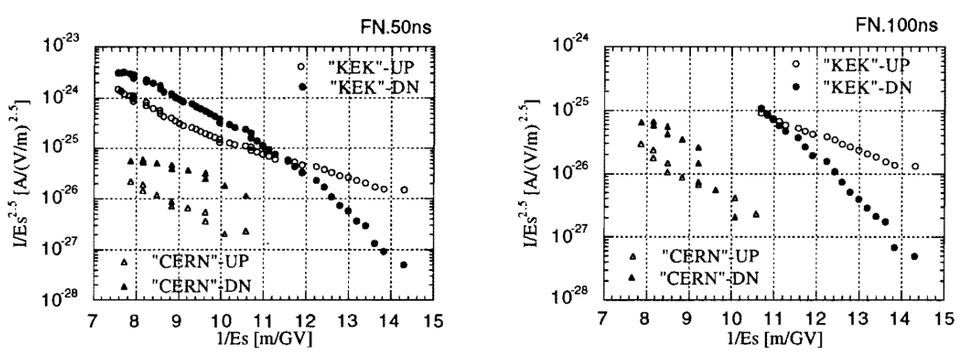

Fig. 15. Modified Fowler-Northeim plot for "KEK" & "CERN" structure at the final stage of the conditioning without pulse compression. The pulse widths are 50ns and 100ns for upper and lower figure, respectively.

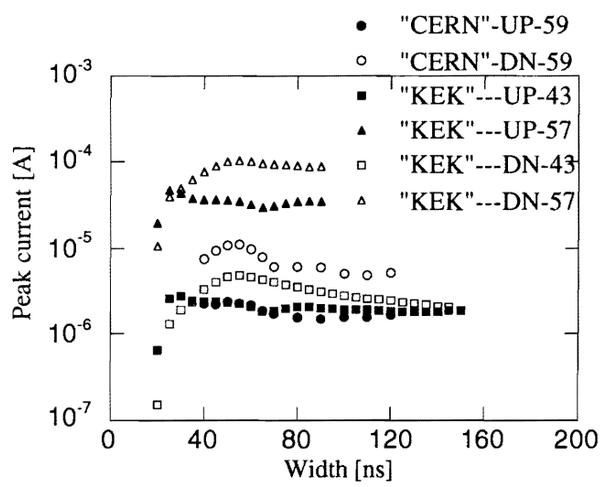

Fig. 16. Peak current versus pulse width. The numbers in the definition of the symbols are the Eav in MV/m.

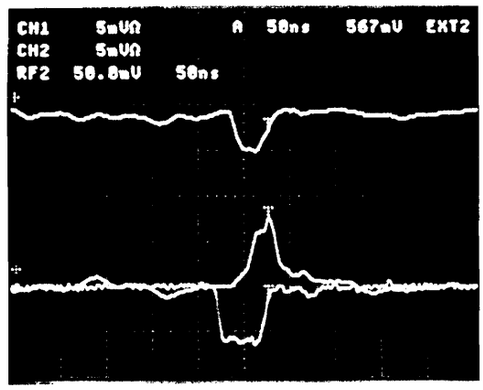

(a) Eav=55 MV/m

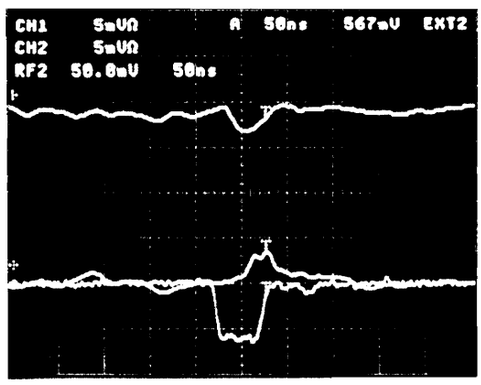

(b) Eav=53 MV/m

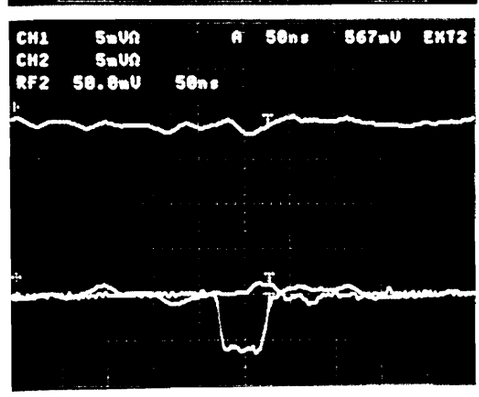

(c) Eav=50 MV/m

Fig. 17. Typical CT output at various field levels measured for "KEK" structure in the middle of the conditioning. Upper and middle (just above the bottom) traces are the current towards upstream and downstream, respectively, while those in the bottom are the input RF pulses. Vertical axis is 1mA/div.

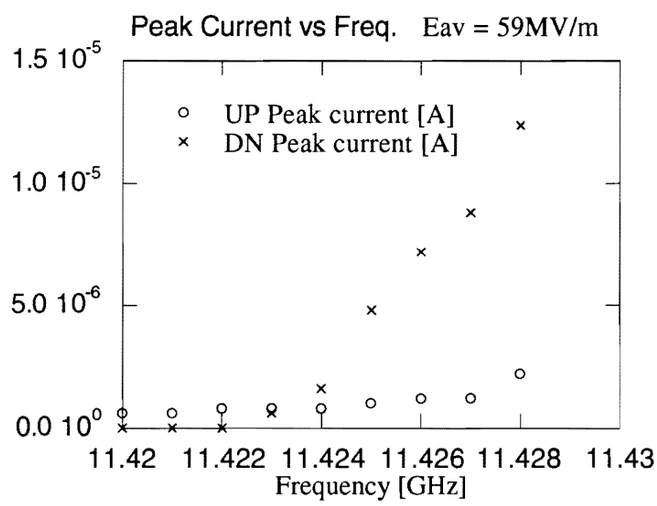

Fig. 18. Dark current versus operating frequency for "CERN" structure at Eav=59MV/m.

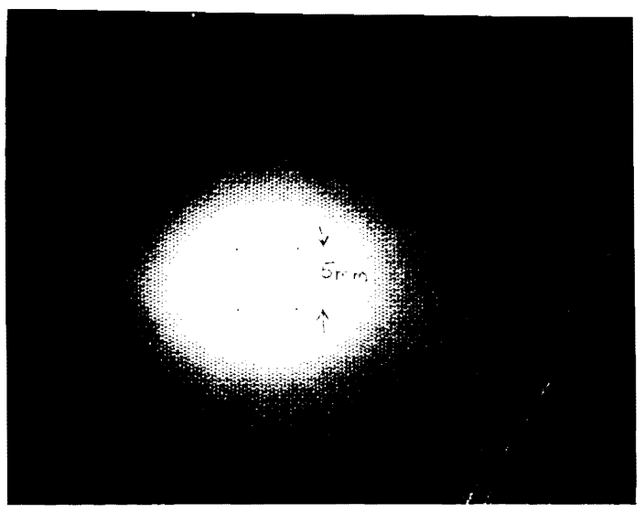

Fig. 19. Typical dark current profile for the case of "CERN" structure with SLED. The distance between each dot in the picture is 5mm.

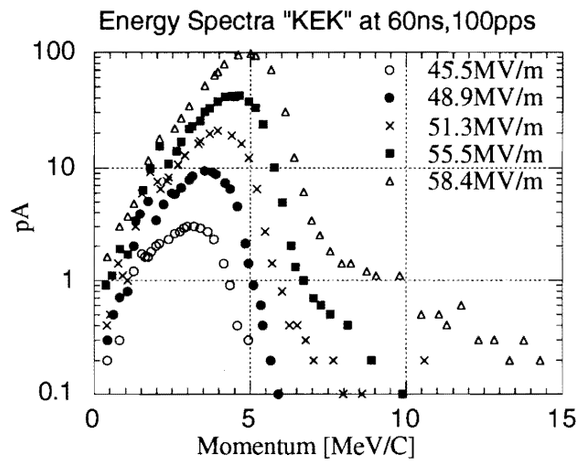

(a)

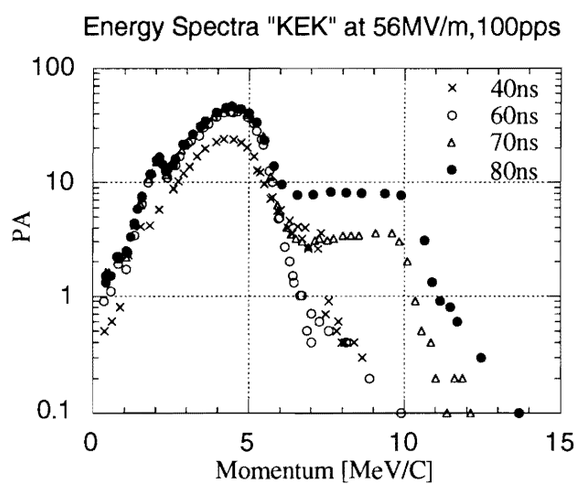

(b)

Fig. 20. Energy spectra of dark current from the "KEK" structure. (a): for pulse width of 60ns at various average field Eav and (b): for Eav=56MV/m at various pulse widths. Momentum acceptance for each bin is 4.3%.

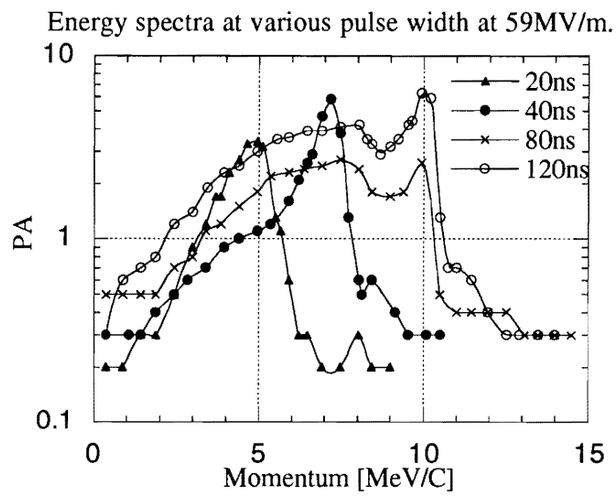

(a)

Fig. 21. Energy spectra of dark current from "CERN" structure for Eav=59MV/m at various pulse widths. Momentum acceptance for each bin is 4.3%.

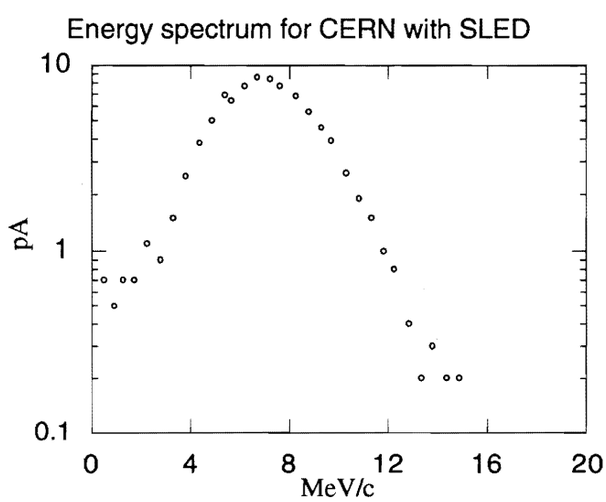

Fig. 22. Energy spectra of dark current from "CERN" structure operated in SLED system at Eav = 72MV/m. Momentum acceptance for each bin is 4.3%.

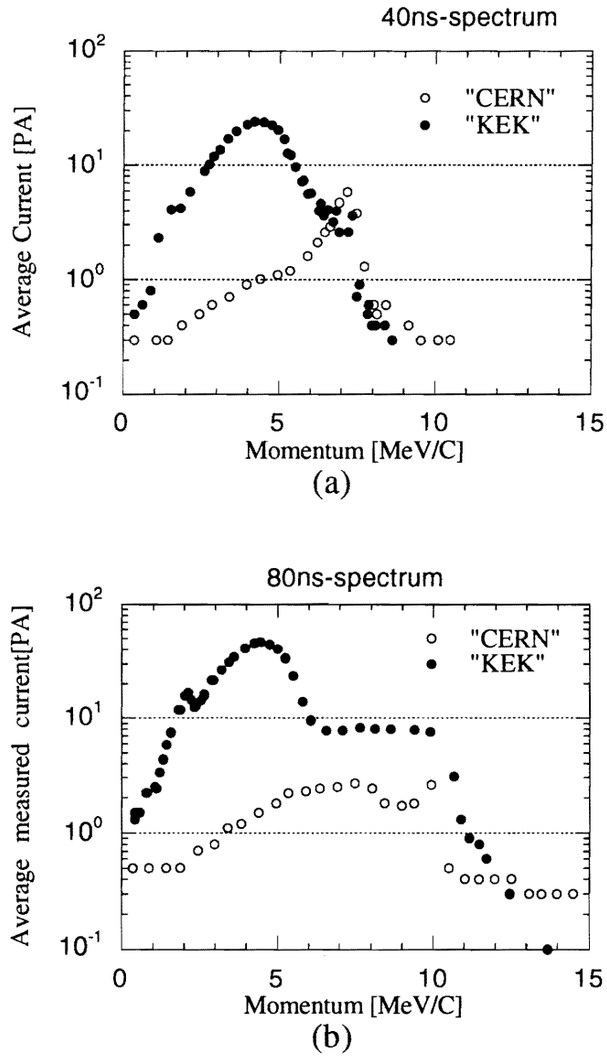

Fig. 23. Comparison of energy spectra for two structures at two pulse widths, below and above the filling time. The average field Eav in the structure was 56MV/m for "KEK" and 59MV/m for "CERN", respectively. The momentum aperture was 4.3%.

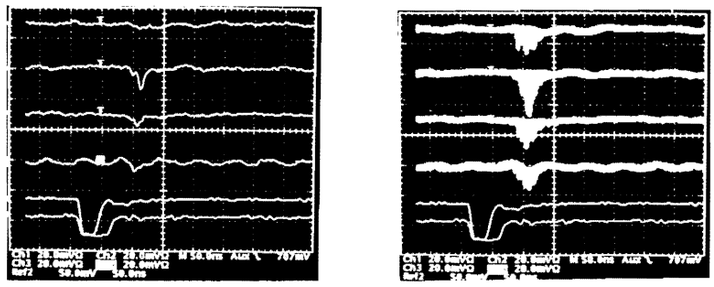

(a) 25ns

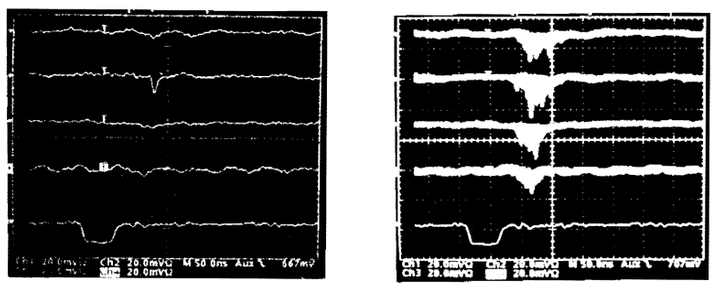

(b) 50ns

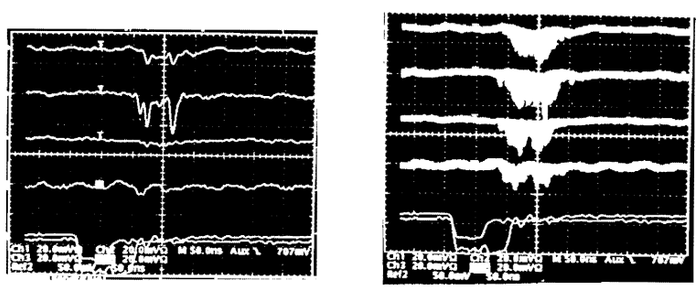

(c) 90ns

Fig. 24. Typical scintillator output pulses measured for "KEK" at the pulse length of (a) 25ns, (b) 50ns and (c) 90ns. Four traces from the top in each picture are those of outputs from SC1, SC2, SC4 and SC5, respectively. The bottom trace shows the timing of the rise of RF input to the stucture. Left figures are a certain snap shot while those in the right are the envelopes of several tens of shots. Note that the scintillator outputs were delayed by 65nsec in the light guide and the photomultiplier.

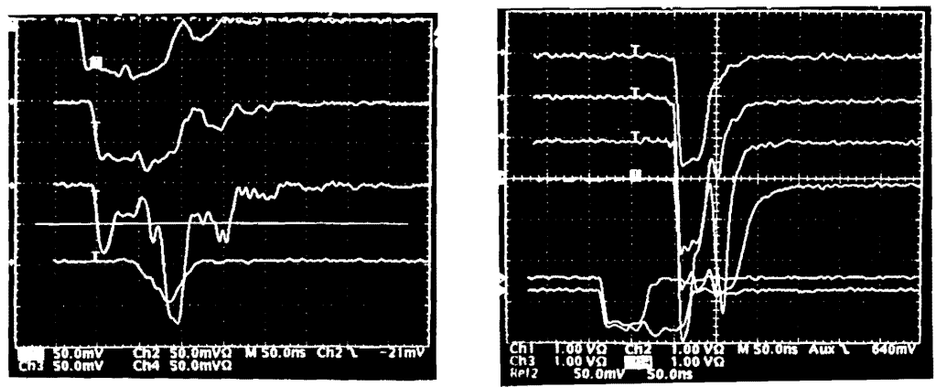

(a) pattern #1

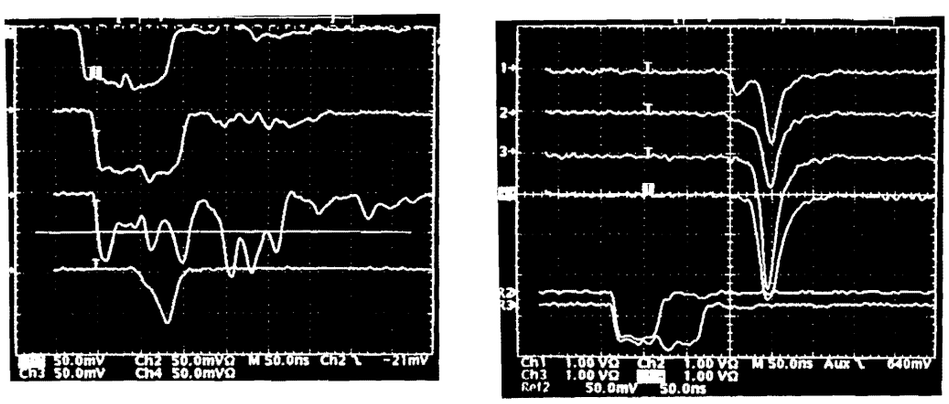

(b) pattern #2

Fig. 25. Two typical breakdown patterns measured for "KEK" structure. Left figures are the RF pulse shapes: klystron output, structure input, reflected from structure and transmitted from structure, respectively, from top to bottom. Those in the right are the scintillator outputs: top four traces are those from scintillators SC1,SC2,SC4 and SC5, while the bottom trace show the input RF timing.

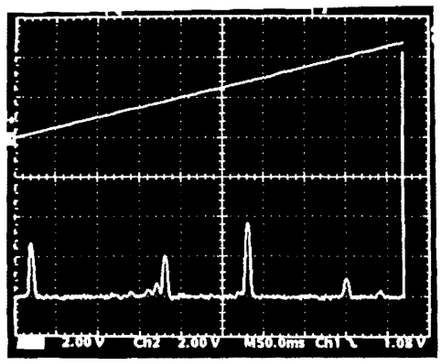

(a) RF off

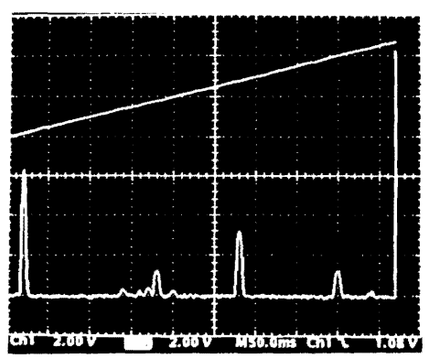

(b) RF on

Fig. 26. Resudual gas components in the "KEK" case measured by QMA after reaching Eav=70MV/m. (a) during RF is off, while (b) RF on. The scale is in linear scale.